NANO LETTERS

2008
Vol. 8, No. 6
1673-1678

# Study of Electron−Phonon Interactions in a Single Molecule Covalently Connected to Two Electrodes

**Joshua Hihath,[†] Carlos R. Arroyo,[‡] Gabino Rubio-Bollinger,[‡] Nongjian Tao,*[,†] and Nicolás Agraït*[,‡]**

*Department of Electrical Engineering, Center for Solid State Electronics, Arizona State University, Tempe, Arizona 85287-5706, and Departamento de Física de la Materia Condensada CIII, Universidad Autónoma de Madrid, E-28049 Madrid, Spain*

*Received February 27, 2008; Revised Manuscript Received April 16, 2008*

**ABSTRACT**

**Presented here is a study of electron−phonon interactions in a single molecule junction where the molecule is covalently connected to two electrodes. In this system, vibration modes in a single molecule junction are measured by sweeping the bias voltage between the two electrodes and recording the differential conductance while the strain in the junction is changed by separating the two electrodes. This unique approach allows changes in conductance to be compared to changes in the configuration of a single molecule junction. This system opens a new door for characterizing single molecule junctions and a better understanding of the relationship between molecular conductance, electron−phonon interactions, and configuration.**

Molecular electronics has shown significant advances in recent years. A variety of interesting effects have been observed including gate effects, rectification, negative differential resistance, and switching.[1] However, despite these advances a detailed understanding of many of the mechanisms involved in molecular electronics has not yet been achieved. To overcome these difficulties, more advanced characterization of molecular scale junctions is needed, to date, several groups have begun to perform inelastic electron tunneling spectroscopy (IETS) on molecular junctions to obtain a chemical signature from the vibration modes of the molecules in the junction.[2–6] However, many of the studies have been done on bulk junctions that take an ensemble average of a large number of molecules in the junction, and in these cases it is not apparent whether the elastic and inelastic contributions to the current come from the same molecules. It has also become possible to measure vibrational spectra on single molecules using scanning tunneling microscopy (STM),[7] an electromigrated junction,[8] a mechanically controlled break junction,[9,10] and in three-terminal devices.[11,12] But in these cases the molecules are not directly connected, it is not possible to probe changes in the molecular configuration or contact geometry, or else the electronic levels of the molecule are so strongly coupled to the electrodes that the conductance is near the conductance quantum, $G_0 = 2e^2/h$. Furthermore, it is well-known that the molecule−electrode contact often plays a dominant role in the transport properties of single molecule junctions, and it is important to probe these differences to better understand what is occurring at the molecular level.[13–15] Therefore, it is necessary to use a method in which two electrodes are covalently bound to the molecule, to be able to separate the electrodes with subangstrøm precision, to know the conductance value of a single molecule junction so that individual molecules can be discriminated, and to probe different molecular junction contact geometries and molecular configurations.

To address these issues we have performed experiments on single molecule junctions using an STM-break junction at cryogenic temperatures. The break junction technique, using either STM or mechanically controlled break junctions (MCBJ), has been intensively used to study atomic contacts in the normal and superconducting states and has served to deepen our understanding of quantum transport at the atomic scale.[16] In particular, it has been established that the conductance of a single-atom junction depends on the chemical nature of the atom and, in the case of gold, is given by $G_0 = 2e^2/h$,[17] and the formation of atomic chains of gold with a conductance of $G_0$ independent of length has been demonstrated.[18] At cryogenic temperatures atomic junctions and chains are very stable making it possible to perform vibrational spectroscopy (IETS).[19] Recently, STM and conducting AFM-break junctions have been used to create

* Corresponding authors: njtao@asu.edu, nicolas.agrait@uam.es.
† Arizona State University.
‡ Universidad Autónoma de Madrid.

10.1021/nl080580e CCC: $40.75 
**Published on Web 05/06/2008**

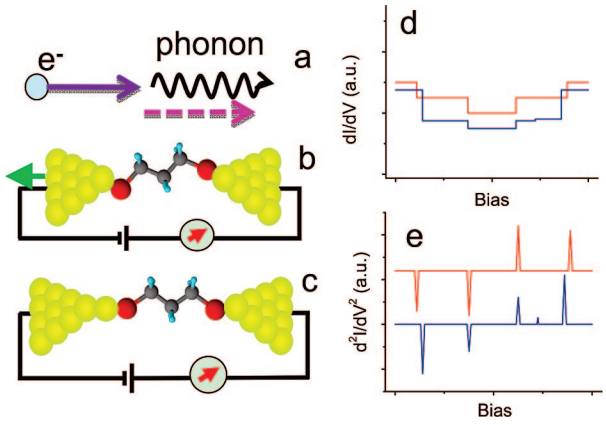


**Figure 1.** Schematic of propanedithiol measurements. (a) Schematic of electron−phonon interaction. While traversing the molecular junction, the electron transfers energy to the molecule as a phonon and continues through the junction at a lower energy. (b) Schematic of measurement system. Once a molecule is held between two electrodes, the differential conductance (d) and phonon spectra (e) are obtained by sweeping the bias and recording the first and second derivatives of the $I-V$ curve (red curves). Then the junction continues to be separated as is shown in (c), until another configuration occurs and the first and second derivative is again recorded in (d) and (e) (blue curves). Thus the phonon spectrum for the molecular junction changes with changes in contact geometry or molecular configuration.

single-molecule junctions covalently bound to the electrodes to provide a statistical analysis of single molecule conductance.[20] Continuing these molecular measurements in the low temperature environment permits very stable molecular junctions and the possibility of performing IETS. This approach, which is repetitive, capable of producing a different contact geometry each time a molecule is contacted, and gives information about that configuration by measuring both the conductance and electron−phonon spectrum, will allow for a better comprehension of the relationship between molecular configuration, contact geometry, and molecular conductance.

In a junction where a single molecule is connected to two gold electrodes, the quantum vibrational modes of the molecule, which at low temperatures and at equilibrium have zero occupation, may be excited by the electrons traversing the molecule. Excitation of a molecular vibration of frequency $\omega$ requires an energy $\hbar\omega$ and consequently an applied bias voltage $V$ larger than the threshold voltage $V_\omega = \hbar\omega/e$. This excitation results in a sudden increase in the differential conductance at the threshold voltage which is observed as a peak in the second derivative of the $I-V$ curve (see Figure 1). It should be noted that this is in contrast to what occurs in gold chains of single atoms where the excitation of a vibrational mode results in a decrease in the conductance.[19] This is a consequence of the difference in conductance of the two systems. Gold chains have an almost completely open single quantum channel with a conductance very close to $1G_0$ and inelastic scattering can only result in backscattering and a decrease in conductance, while for molecules conductance channels are almost completely closed and inelastic scattering enhances the conductance.[21,22]

To demonstrate the measurement of vibrational spectroscopy in a single molecule bound to two electrodes, a short alkane chain was chosen as a model system, 1,3-propanedithiol. This molecule was chosen as a test case since the conductance of alkanedithiols has been widely studied in the literature,[14,15,20,23,24] and this short molecule provides a large current which can be easily measured experimentally. In order to accurately measure a signature from electron−phonon interactions in a single molecule, it is first necessary to determine the conductance of a single molecule. The conductance was found using a standard STM-break junction[20] approach using a low-temperature STM previously described elsewhere.[25] In this method, measurements are carried out by pressing the STM tip into the gold surface and monitoring the current while withdrawing the tip. In cases where molecules are attached between the tip and the surface, steps will occur in the conductance decay below $G_0$. These steps will give a peak in the conductance histogram at the most probable conductance of a single molecule junction. After several thousand curves were recorded, a conductance histogram was constructed by taking the logarithm of each curve and sampling the resulting curve with a fixed bin size. Adding all of the curves together resulted in histograms with a broad peak at $(6 \times 10^{-3})G_0$. The conductance can also be predicted using a simple tunneling model, $G = Ae^{-(\beta N)}$, where $\beta$ is the decay constant, $A$ is the effective contact conductance, and $N$ is the number of carbon atoms in the chain. For alkane chains these values have been previously measured as $\beta = 1.08/N$ and $A = 0.22G_0$,[13] this model predicts a conductance of $(8 \times 10^{-3})G_0$ for propanedithiol, similar to the value measured. A representative histogram at 50 mV bias taken from 3000 curves without selection is shown in Figure 2a; this histogram has a dominate peak at $G_0$ indicating a gold−gold contact, and a clear peak is also visible at $(6 \times 10^{-3})G_0$, which has been attributed to a propanedithiol junction.

After the conductance of the molecule is known, it is then possible to proceed with electron−phonon interaction studies. To record inelastic electron tunneling (IET) spectra, the tip was contacted to the surface and then withdrawn until a conductance plateau became apparent. At this point, withdrawal of the tip was paused and the bias swept. The resulting $I-V$ curve was recorded, as well as either the first or second derivative, using a standard ac modulation and lock-in amplifier technique.[26] In cases where the first derivative was recorded with the lock-in amplifier, the spectra were obtained by taking the numerical derivative and using a Savitzky−Golay filter to remove noise generated from the numerical derivative. After a spectrum was recorded, the tip withdrawal continued in small steps, and additional spectra were recorded at various distances along the conductance trace until the junction eventually broke. Using this scheme it is possible to see how the spectra change with changes in the conductance of the molecular junction. One junction with spectra shown at several places along the curve is shown in Figure 2. The individual spectra on this plateau are quite similar. Since there is little change in the spectra along a plateau in the conductance decay, it is possible to average the curves

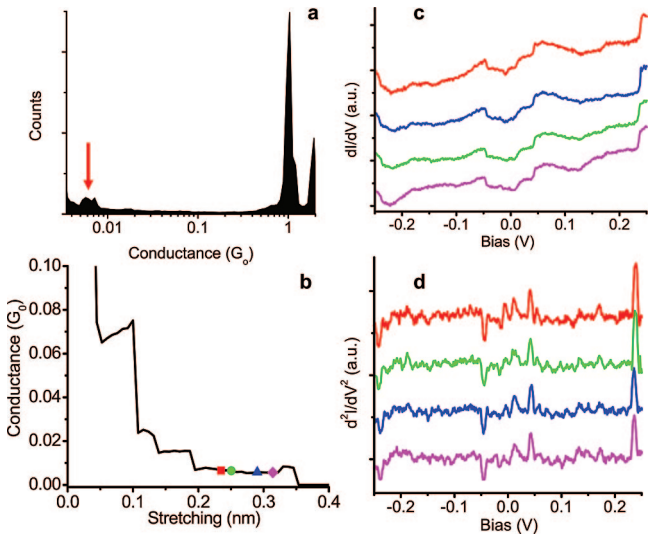


**Figure 2.** Single molecule IETS measurement. (a) Semilog conductance histogram with a peak at $G_0$, and an additional peak at $(6 \times 10^{-3})G_0$, which is attributed to the conductance of propanedithiol. (b) A conductance curve with steps for a single molecule measurement. The four symbols represent four stretching distances where the bias was swept and the $I-V$ and first derivate were recorded. (c) The corresponding four first derivative curves (offset for clarity), and (d) the corresponding IET spectra obtained numerically. The curves are antisymmetric, and certain features are very reproducible along the conductance plateau.

in that region to decrease the noise without significantly broadening the peaks in the spectra and obtain the average spectrum for a junction or conductance plateau.

In the analysis of the IET spectra it is essential to extract the features that correspond to the excitation of the molecular vibrations (inelastic scattering). Electronic and mechanical noise yield features that are not reproducible and which are reduced using lock-in amplification techniques and averaging. The most important effect in the experimental curves is that due to elastic scattering of the electrons in the electrodes with defects or impurities results in interference effects, the so-called conductance fluctuations,[16] which result in large features in the conductance curves which are typically not symmetric. Since these fluctuations have its origins mainly in the electrodes, the resulting features do not change much during elastic deformation of the junction. In contrast, features due to the excitation of the molecular vibrations are symmetric in the conductance or antisymmetric in its derivative, the IET spectrum. We will focus on these antisymmetric features in the IET spectra.

In the process of performing IET spectroscopy, 155 junctions were measured. This data set included 13 junctions where 10 or more first derivative curves were recorded before breaking. The rest of the junctions either measured the second derivative directly or broke before 10 $I-V$ sweeps were completed. These 13 junctions provided a total of 448 spectra with ±200 mV range or greater. All of these spectra were used as a data set for determining phonon modes. Also, it should be noted that although these modes are antisymmetric in the IET spectra, all counts are added positively to the phonon histogram, thus creating a symmetric graph. To determine if the features in the spectra are antisymmetric, a LabView program was written to determine the peak positions in the IET spectra. The process to make this determination entailed comparing all negative peaks found in the negative bias region with all positive peaks in the positive bias region for each IET spectrum. If a negative peak in the negative bias region was within 5% of a positive peak in the positive bias region, then both peaks were added to the phonon modes histogram as a single count; as such, only antisymmetric features were included in this histogram. This process was completed for all spectra with a bias range greater than ±200 mV for the 13 junctions, and the resulting phonon histogram is shown in Figure 3a. A histogram including all peaks from the IET spectra, whether antisymmetric or not, produced a histogram with features at the same energies as in the previous case, although the background is larger in this histogram, as is shown in Figure 3b. Both histograms in Figure 3 have several obvious peaks, and these peaks show that there are certain modes in the low-energy regime that are quite clear and repeatable across junctions. There is a distribution for each peak, indicating that significant shifts in energy can occur for these modes either across or even within junctions. Also, the histograms in Figure 3 show some counts that do not produce clear peaks indicating that there may be other phonon modes that are not as pronounced in the molecular junctions. Nonetheless, there is a significant amount of information that can be gleaned from the clear peaks in the histogram.

There are several clear modes visible, and many possible modes below 250 mV; this is in contrast to some of the experiments done on alkanes where the zero bias feature dominates most of the low-frequency modes.[3] However, these spectra do show some similarity to the results obtained using a nanopore configuration for a bulk junction.[4] Table 1 lists all of the modes observed in the phonon modes histogram. Since alkanethiols have been studied a great deal with both optical and electron energy loss spectroscopies, it is possible to assign several peaks from the literature.[27–31] However, since this is a special case where both ends are anchored, a model was used to help determine which vibration modes occur in the histogram. A simple one-dimensional model similar to that found repeatedly in the literature for determining longitudinal accordion modes (LAM) was used, where each atom in the chain is represented by a mass and spring.[32–35] In this case, a Au atom is anchored at each end, and a Au−S−C−C−C−S−Au structure is placed between the two end points. The masses for the atoms were 197 amu for Au, 32 amu for sulfur, and 14 amu for each $CH_2$ unit. Spring constants were obtained from the literature. AuS and CS values were obtained from Levin et al.[33] as 1.2 and 2.49 mdyn/Å, respectively, the C−C value was obtained as 5.2 mdyn/Å from Minoni et al.,[34] and the Au−Au spring constant used was 0.08 mdyn/Å.[36] Finding the eigenvalues and eigenvectors from the resulting matrix produced vibration modes with energies of 4, 11, 26, 48, 73, 123, and 176 meV, in excellent agreement with many of the peaks observed in the histograms in Figure 3. The values from the model that are not apparent in the histogram are at 4 and 26 meV, due largely to the Au−Au and Au−S

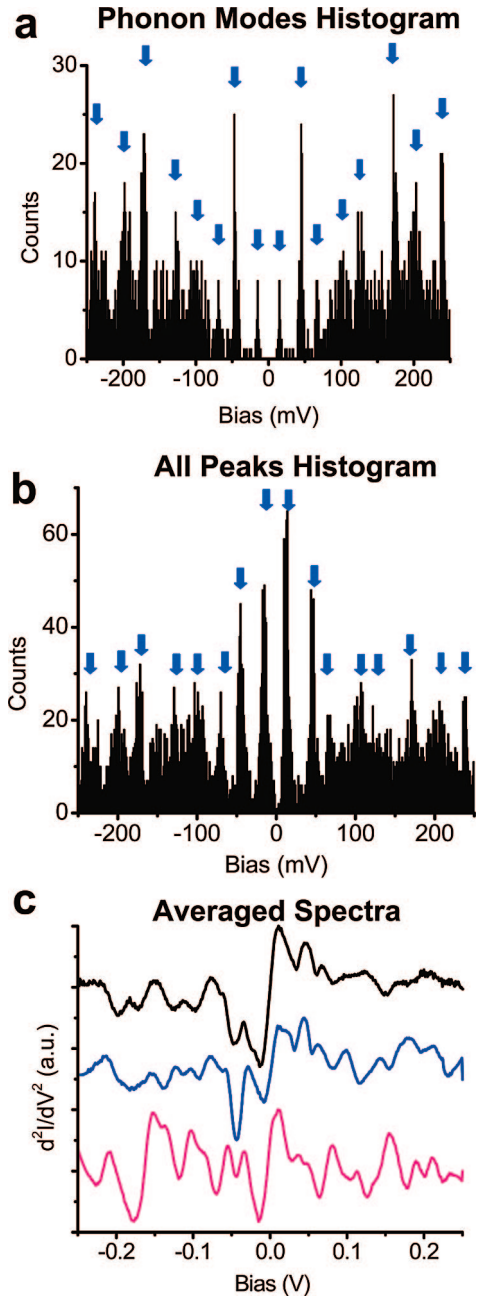


**Figure 3.** Analysis of phonon modes from the IET spectra. (a) A histogram of all antisymmetric peaks from 448 IET spectra across 13 separate junctions. There are several clear peaks in the histogram that can be matched from a simple model or by comparison with optical measurements. (b) Peak histogram from all peaks in the IET spectra (regardless of symmetry). Histogram b shows the same behavior as histogram a, but with a larger distribution. (c) Examples of averaged spectra from three different junctions. Several modes are consistent across junctions despite changes in intensity.

stretch modes. These modes are likely hidden by the often dominant 15 mV mode. The other modes involve a combination of various bonds in the molecular junction but are often dominated by a single bond. Although Table 1 lists only the dominate mode, it should be noted that many of the bonds couple for each of the modes listed. Furthermore, even though the model is purely longitudinal, the values from literature represent an effective spring constant, and as such the zigzag shape of the molecule requires that these modes involve both a bend and stretch component. The additional peak at 100 mV is likely due to a $CH_2$ rock,[30,31] which the model is not capable of capturing. Similarly, the modes at 201 and 237mV are difficult to assign either with this model or by comparison with the literature since they do not appear to be active in IR or Raman spectra. Nevertheless, from this analysis, it is possible to infer that the electrons interact strongly with the tunneling pathway and, therefore, the molecular backbone, as has been predicted in several theoretical models.[37–40]

This strong interaction with the molecular backbone lends itself to a unique opportunity to examine configuration changes in a single molecule junction. The phonon mode histogram (Figure 3) shows a clear distribution in the modes. However, it is not obvious whether this distribution comes from changes between junctions or if the modes can change significantly while the junction is being separated. As stated above, and shown in Figure 2, the changes that occur along a conductance plateau are small which is likely due to stretching taking place at the Au contacts.[41,42] However, when the spectra are compared across different plateaus within a junction, the changes can be quite striking. Since the changes in spectra along the plateau are small, the spectra from several bias sweeps on a plateau are averaged to reduce the noise in the individual spectra. Then, by considering the averaged spectra from different regions in the conductance decay, it is possible look for changes in the known modes as the junction evolves. Figure 4 shows one example, here the red curve corresponds to an average of 20 spectra on one plateau when the junction first forms and the blue spectrum is an average of 20 spectra from a later plateau level in the decay. In these spectra only the low-frequency regime is considered, and at the 46 mV peak, which was so apparent in the phonon histogram, it is clear that this mode can change significantly in both position and intensity as the junction evolves and the conductance changes. In this case, the energy of the mode changed from 42 to 46 mV. This dramatic change occurs along the backbone of the molecular junction and involves CS, AuS, and AuAu bonds. Such a change could occur due to either a change in the contact configuration or a change between gauche and trans configurations in the molecular junction.[29] Nevertheless, this shift clearly illustrates the impact of the junction configuration on the conductance of the molecule. With such clear changes in the energy of the modes, this method could be extremely important in molecular electronics to help elucidate the interplay between the contact, molecular configurations, and the conductance behavior of a single molecule junction.

In conclusion, it is possible to measure electron−phonon interactions in a single molecule covalently bound to two electrodes. For propanedithiol, a series of phonon modes are observed, and these modes match well with IR and Raman spectra and have been described by a simple one-dimensional model. Although there can be significant differences in the spectra of different junctions, this difference provides an opportunity to look at different contact geometries and configuration differences between molecular junctions, while a statistical analysis provides information about which

**Table 1.** Peaks from the Histogram in Figure 3a and Corresponding Mode Assignments[a]

| Negative Bias (mV) | Positive Bias (mV) | Wavenumber ($cm^{-1}$) | Literature Values [19, 27-31] (meV) | Calculated Energy (meV) | Peak Assignment | Mode Movement |
|---|---|---|---|---|---|---|
| -238 | 237 | 1936 | | | | |
| -198 | 201 | 1613 | | | | |
| -171 | 172 | 1387 | | 176 | $\nu_a$CC | |
| -127 | 126 | 1000 | 126-13 | 123 | $\nu_s$CC | |
| -100 | 100 | 798 | 89-97 | | $\rho CH_2$ | |
| -69 | 67 | 556 | 74-89 | 73 | $\nu_a$CS | |
| -46 | 46 | 371 | 42-50 | 48 | $\nu_s$CS | |
| -15 | 15 | 120 | 12-20 | 10 | vAuAu | |

[a] $\nu$ denotes a stretch mode. $\rho$ denotes a rocking mode. Subscripts s and a denote symmetric and antisymmetric modes.

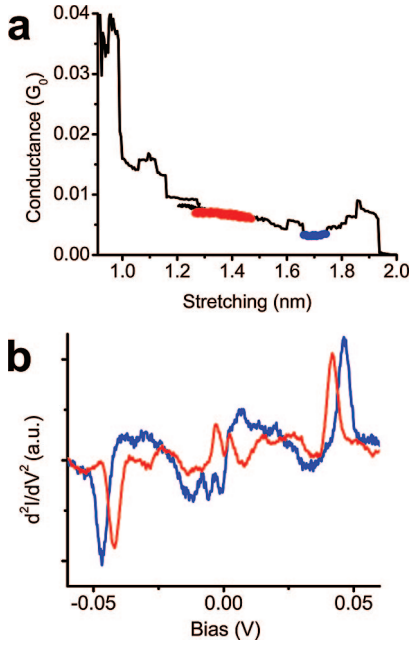


**Figure 4.** Correlation of changes in vibration modes and conductance. (a) Conductance change of a junction during stretching. The red and blue areas in the conductance decay show the regions over which the spectra were averaged. (b) Two spectra where the conductance is locally constant. The two regions show a clear shift in the mode at 46 mV which corresponds to a coupled AuS, CS mode in the molecular junction. This shift demonstrates a clear correlation between changes in the IET spectrum, the molecular junction conductance, and the junction configuration.

features can be considered phonons modes and which are due to conductance fluctuations. Furthermore, since it is possible to dynamically change the configuration of the junction in this system by separating the two electrodes while recording spectra, it is possible to see simultaneous changes in the conductance and vibration modes of a single molecule as the junction is stretched. This method allows for a better understanding of the roles of molecular configuration, contact geometry, and strain on the conductance in a single molecule junction by looking at how the vibration modes in the spectra change and could prove to be a useful tool for characterizing single molecule electronics.

**Acknowledgment.** This work was supported by DOE (DE-FG03-01ER45943, N.J.T.), NSF (CHM-0554786, J.H.), and Spanish MEC (MAT2004-03069 and CONSOLIDER CSD2007-0010) and CAM (Citecnomik, P-ESP-0337-0505).

## References

(1) Tao, N. J. *Nat. Nanotechnol.* **2006**, *1* (3), 173–181.
(2) Jaklevic, R. C.; Lambe, J. *Phys. Rev. Lett.* **1966**, *17* (22), 1139–1140.
(3) Kushmerick, J. G.; Lazorcik, J.; Patterson, C. H.; Shashidhar, R.; Seferos, D. S.; Bazan, G. C. *Nano Lett.* **2004**, *4* (4), 639–642.
(4) Wang, W.; Lee, T.; Kretzschmar, I.; Reed, M. A. *Nano Lett.* **2004**, *4* (4), 643–646.
(5) Di Ventra, M.; Kim, S. G.; Pantelides, S. T.; Lang, N. D. *Phys. Rev. Lett.* **2001**, *86*, 288–291.
(6) Troisi, A.; Ratner, M. A. *Nano Lett.* **2006**, *6* (8), 1784–1788.
(7) Stipe, B. C.; Rezaei, M. A.; Ho, W. *Science* **1998**, *280* (5370), 1732–1735.
(8) Yu, L. H.; Keane, Z. K.; Ciszek, J. W.; Cheng, L.; Stewart, M. P.; Tour, J. M.; Natelson, D. *Phys. Rev. Lett.* **2004**, *93* (26, part 1), 266802/1–266802/4.
(9) Thijssen, W. H. A.; Djukic, D.; Otte, A. F.; Bremmer, R. H.; van Ruitenbeek, J. M.*Phys. Rev. Lett.* **2006**, *97* (22), 226806/1–226806/4.
(10) Djukic, D.; Thygesen, K. S.; Untiedt, C.; Smit, R. H. M.; Jacobsen, K. W.; van Ruitenbeek, J. M. *Phys. Rev. B: Condens. Matter Mater. Phys.* **2005**, *71* (16), 161402/1–161402/4.
(11) Osorio, E. A.; O'Neill, K.; Stuhr-Hansen, N.; Nielsen, O. F.; Bjornholm, T.; van der Zant, H. S. J. *Adv. Mater. (Weinheim, Ger.)* **2007**, *19* (2), 281–285.
(12) Park, H.; Park, J.; Lim, A. K. L.; Anderson, E. H.; Alivisatos, A. P.; McEuen, P. L. *Nature (London)* **2000**, *407* (6800), 58–60.
(13) Chen, F.; Li, X.; Hihath, J.; Huang, Z.; Tao, N. *J. Am. Chem. Soc.* **2006**, *128* (49), 15874–15881.
(14) Li, C.; Pobelov, I.; Wandlowski, T.; Bagrets, A.; Arnold, A.; Evers, F. *J. Am. Chem. Soc.* **2008**, *130* (1), 318–326.
(15) Li, X.; He, J.; Hihath, J.; Xu, B.; Lindsay, S. M.; Tao, N. *J. Am. Chem. Soc.* **2006**, *128* (6), 2135–2141.
(16) Agrait, N.; Yeyati, A. L.; van Ruitenbeek, J. M. *Phys. Rep.* **2003**, *377* (2−3), 81–279.
(17) Scheer, E.; Agrait, N.; Cuevas, J. C.; Yeyati, A. L.; Ludoph, B.; Martin-Rodero, A.; Bollinger, G. R.; van Ruitenbeek, J. M.; Urbina, C. *Nature* **1998**, *394* (6689), 154–157.
(18) Yanson, A. I.; Bollinger, G. R.; Van Den Brom, H. E.; Agrait, N.; Van Ruitenbeek, J. M. *Nature (London)* **1998**, *395* (6704), 783–785.
(19) Agrait, N.; Untiedt, C.; Rubio-Bollinger, G.; Vieira, S. *Phys. Rev. Lett.* **2002**, *88* (21), 216803/1–216803/4.
(20) Xu, B.; Tao, N. J. *Science* **2003**, *301* (5637), 1221–1223.

(21) Paulsson, M.; Frederiksen, T.; Brandbyge, M. *Phys. Rev. B: Condens. Matter Mater. Phys.* **2005**, *72* (20), 201101/1–201101/4.
(22) de la Vega, L.; Martin-Rodero, A.; Agrait, N.; Yeyati, A. L. *Phys. Rev. B: Condens. Matter Mater. Phys.* **2006**, *73* (7), 075428/1–075428/5.
(23) Gonzalez, M. T.; Wu, S.; Huber, R.; van der Molen Sense, J.; Schonenberger, C.; Calame, M. *Nano Lett.* **2006**, *6* (10), 2238–42.
(24) Jang, S.-Y.; Reddy, P.; Majumdar, A.; Segalman, R. A. *Nano Lett.* **2006**, *6* (10), 2362–2367.
(25) Agrait, N.; Rodrigo, J. G.; Viera, S. *Phys. Rev. B: Condens. Matter Mater. Phys.* **1992**, *46* (9), 5814–5817.
(26) Petit, C.; Salace, G. *Rev. Sci. Instrum.* **2003**, *74* (10), 4462–4467.
(27) Nandy, S. K.; Mukherjee, D. K.; Roy, S. B.; Kastha, G. S. *J. Phys. Chem. A* **1973**, *77* (4), 469–71.
(28) Bryant, M. A.; Pemberton, J. E. *J. Am. Chem. Soc.* **1991**, *113* (22), 8284–93.
(29) Joo, S. W.; Han, S. W.; Kim, K. *J. Phys. Chem. B* **2000**, *104* (26), 6218–6224.
(30) Kato, H. S.; Noh, J.; Hara, M.; Kawai, M. *J. Phys. Chem. B* **2002**, *106* (37), 9655–9658.
(31) Roeges, N. P. G. *A Guide to the Complete Interpretation of Infrared Spectra of Organic Structures*, 1st ed.; John Wiley & Sons Ltd.: Chichester, West Sussex, England, 1994; Vol. 1, p 340.
(32) Schaufele, R. F.; Shimanouchi, T. *J. Chem. Phys.* **1967**, *47* (9), 3605–10.
(33) Levin, C. S.; Janesko, B. G.; Bardhan, R.; Scuseria, G. E.; Hartgerink, J. D.; Halas, N. J. *Nano Lett.* **2006**, *6* (11), 2617–2621.
(34) Minoni, G.; Zerbi, G. *J. Phys. Chem.* **1982**, *86* (24), 4791–8.
(35) Wilson, E. B.; Decius, J. C.; Cross, P. C. *Molecular Vibrations, The Theory of Infrared and Raman Vibrational Spectra*, 1st ed.; McGraw-Hill: New York, 1955; p 388.
(36) Xu, B. Q.; He, H. X.; Boussaad, S.; Tao, N. J. *Electrochim. Acta* **2003**, *48* (20−22), 3085–3091.
(37) Troisi, A.; Beebe, J. M.; Picraux, L. B.; van Zee, R. D.; Stewart, D. R.; Ratner, M. A.; Kushmerick, J. G. *Proc. Natl. Acad. Sci. U.S.A.* **2007**, *104* (36), 14255–14259, S14255/1−S14255/4.
(38) Troisi, A.; Ratner, M. A. *Phys. Chem. Chem. Phys.* **2007**, *9* (19), 2421–2427.
(39) Chen, Y.-C.; Zwolak, M.; Di Ventra, M. *Nano Lett.* **2005**, *5* (4), 621–624.
(40) Solomon, G. C.; Gagliardi, A.; Pecchia, A.; Frauenheim, T.; Di Carlo, A.; Reimers, J. R.; Hush, N. S. *J. Chem. Phys.* **2006**, *124* (9), 094704/1–094704/10.
(41) Huang, Z.; Chen, F.; Bennett, P. A.; Tao, N. *J. Am. Chem. Soc.* **2007**, *129* (43), 13225–13231.
(42) Xu, B.; Xiao, X.; Tao, N. J. *J. Am. Chem. Soc.* **2003**, *125* (52), 16164–16165.

NL080580E